F. J. Asensio, J. I. San Martín, I. Zamora, O. Oñederra, G. Saldaña and M. González, "*Optimal sizing and operation methodology for the on-board electrical generation and energy recovery system of an aircraft*," **IECON 2020 The 46th Annual Conference of the IEEE Industrial Electronics Society**, Singapore, 2020, pp. 4277-4282, doi: 10.1109/IECON43393.2020.9254937.

Optimal sizing and operation methodology for the on-board electrical generation and energy recovery system of an aircraft

F.J. Asensio[1], J.I. San Martín[1], I. Zamora[2], O. Oñederra[2], G. Saldaña[1], M. González[1]
Department of Electrical Engineering – University of The Basque Country (UPV/EHU)

[1]Engineering Schoool of Gipuzkoa
Avda. Otaola, 29, 20600 Eibar (Spain)
franciscojavier.asensio@ehu.eus

[2]Engineering School of Bilbao
Alda. Urquijo s/n, 48013 Bilbao (Spain)
inmaculada.zamora@ehu.eus

Abstract—This paper focuses on a novel sizing and operation methodology for the on-board electrical generation and energy recovery system of an aircraft. The proposed operation methodology lies in the optimal management of a hydrogen fuel cell to support on-board power generation and the traction system during taxiing. In addition to the on-board generation system, the operation methodology also contemplates energy recovery by regenerative braking during landing, through the use of reversible electric machines and lithium-ion cells. The sizing methodology allows choosing the optimal number, power and / or capacity of the hydrogen tank, fuel cells, reversible electric machines and lithium-ion cells of which the microgrid is composed. In this sense, the sizing methodology considers technical aspects, such as the on-board energy requirements, sanitary water requirements, available regenerative energy, and weight of all devices, among others. Besides, power conversion structures and control topologies are proposed for the microgrid optimal operation. After simulating the system in the MATLAB environment, it has been verified that the proposed methodology allows reducing the weight of the airplane at takeoff, increasing energy efficiency, which leads to a net savage of 14,070 €/year per aircraft.

Keywords—More Electric Aircraft (MEA), Operation methodology, On-board generation, Proton Exchange Membrane Fuel Cell (PEMFC), Lithium-ion cell.

I. INTRODUCTION

Demand for air transport for both passenger and cargo has more than doubled since 2000, and it is expected to continue growing by just under 5% per year for the next two decades [1]. This growth will have environmental consequences via noise, air quality and climate impacts. In this sense, nowadays, the air transport sector is responsible for approximately 2.5% of CO_2 emissions worldwide, from which the passenger transport accounts for 81% of the total, and considering the most recent forecasts, this scenario is expected to double by 2050 [2], [3].

There are several potential methods to mitigate these effects, such as regulations and standards, market-based policies, the development of sustainable fuels, operational improvements, and energy efficiency improvements involving airplane and turbojet performance. In this context, the aviation sector has achieved substantial improvements in terms of energy efficiency, having improved by 2.9% per year during the period 2000-2016 [4]. Within the short-term horizon, several aims have been set for energy efficiency improvements and CO_2 emissions reduction for local aviation by the United Nations Framework Convention on Climate Change (UNFCCC), the Kyoto protocol and the Paris Agreement, and for international aviation by the International Civil Aviation Organization (ICAO) [4]. In this sense, the ICAO has adopted a resolution to achieve an energy efficiency improvement of 2% per year until 2050. Regarding CO_2 emissions, the ICAO has adopted the Carbon Offsetting and Reduction Scheme for International Aviation (CORSIA) initiative, which establishes that from 2021 the aviation industry will achieve carbon neutral growth [4]. In this sense, international flights that have higher emission rates will have to compensate them through carbon offsetting. In addition, to guide the aviation sector towards the Sustainable Development Scenario (SDS), it is necessary to reduce specific energy consumption by more than 3% per year until 2030 [5].

In current literature, several research works aimed at improving energy efficiency in aviation can be found. In this sense, focusing on the electrical and electronic scope, some proposals include designs of more efficient electronic converters, based on Gallium nitride (GaN), on cryogenic cooling that allows higher switching frequency, or on optimized designs that reduce the number of necessary components [6], [7], [8]. Other proposals focus on electric machine improvements, reducing windings losses by novel asymmetric configurations, by minimizing the active material or by replacing them by ones based on superconducting materials [9], [10], [11]. Optimal energy management and energy recovery is another approach by which efficiency can be improved, such as by using Energy Storage Systems (ESS) based on supercapacitors or batteries. [12].

Leaving aside the improvement of existing components, other way to approach the improvement of energy efficiency in aviation sector lies in the use of more efficient power generation technologies. In this sense, Proton Exchange Membrane Fuel Cells (PEMFC) become a very suitable solution due to their high efficiency, power density, low weight and noise, and zero emissions when they are fed with hydrogen [13]. Besides, in case of hybridizing a PEMFC system with an ESS based on lithium-ion cells, this favor the dynamics of the system allowing it to respond quickly to increases in electricity demand [14].

Considering all above mentioned, this paper proposes a lithium-ion cells and PEMFC-based microgrid configuration for on-board electrical generation and energy recovery of an aircraft. In addition, an optimal sizing and operation methodology aimed at reducing operational costs and CO_2 emissions and at improving the energy efficiency is presented. Finally, the developed methodology is applied by way of example on a commercial passenger airplane.

II. Microgrid System Description

The electrical microgrid of the aircraft is comprised of a PEMFC system, a Lithium-ion battery, Permanent Magnet Synchronous Generators (PMSG), reversible Permanent Magnet Synchronous Machines (PMSM), electrical loads and the electronic converters used to couple all the devices into the DC link and to optimally manage all the power flows that will occur in the different modes of operation. Fig. 1 shows a scheme of the configuration of the proposed microgrid system.

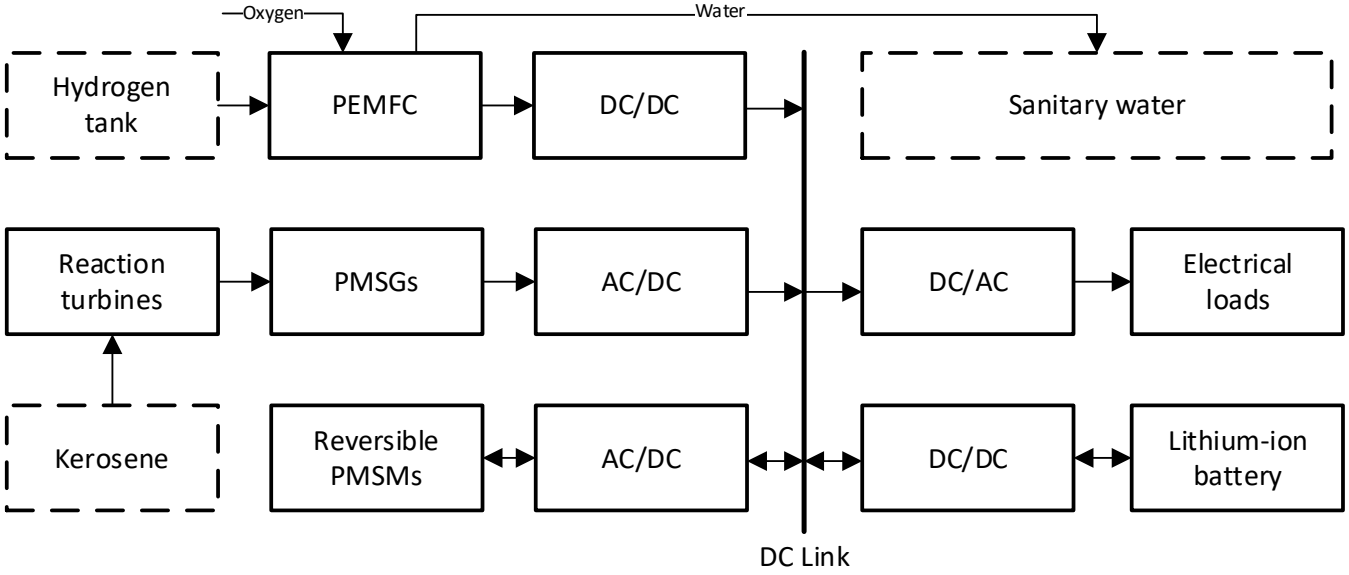

Fig. 1. Configuration of the proposed microgrid for the airplane.

Following the function of each power generation and storage device, as well as the topology of the power electronic converters associated with each device are described:

- The PEMFC system is fed by hydrogen previously stored in the hydrogen tank and is used to provide electrical power during flight and taxiing operations. The water obtained as a by-product of electrochemical reactions is stored in a tank for later use. The fuel cell is connected to the DC link through a boost converter.
- PMSGs are coupled to the turbojets and are used to provide electrical power during flight and taxiing operations. These are connected to the DC link through three phase full-wave diode bridge rectifiers and boost converters.
- The reversible PMSMs located in the landing gear are in-wheel type and are used during taxiing (motor mode) and landing (generator mode) operations. These are connected to the DC link through a voltage type three-phase IGBT full-bridge inverters and bidirectional buck-boost converters, which are responsible for managing the PMSMs to move the aircraft on the runway and for managing the energy recovered during braking on landing.
- The lithium-ion cell-based battery is used to store the energy recovered at landing and to provide energy during the taxiing operation. It is connected to the DC link through a bidirectional buck-boost converter.
- The electric loads represent the electrical consumption of the aircraft, such as entertainment systems, lighting, control systems, etc. For this case, it has been assumed that all electrical energy consumption is in AC.

III. Operation Methodology

In addition to the jet fuel needed to boost and brake an aircraft, more fuel is also required to supply the electrical energy demand of the aircraft during the flight, which is produced by electrical machines coupled to the turbojets. Turbojets are usually located on wings in the case of all large commercial aircrafts, which are designed to operate optimally at a certain speed, temperature, air pressure, and altitude, which are met when the aircraft is flying at cruising speed. In this context, when the aircraft operates in taxiing mode on track, its reactors usually operate at idle speed, and since they are not designed to operate at land conditions, energetic efficiency is drastically reduced during taxiing operation.

With jet fuel accounting for around 20% of aviation operating costs in 2018, airlines are pursuing an improvement in energy efficiency in order to maximize their benefits [15]. In this sense, below, three modes of operation are described to rise the efficiency by optimally managing the energy flows of the microgrid during flight, taxiing and landing operation modes. For each operation mode, the resulting scheme is described, including the description of the control topology implemented for each power electronic device.

A. System Operation during Flight

During flight operation mode, both PEMFC and PMSGs coupled to the turbojets provide electrical power to meet the electrical demand of the aircraft. Fig. 2 shows the conversion stage used to connect the PEMFC to the DC link.

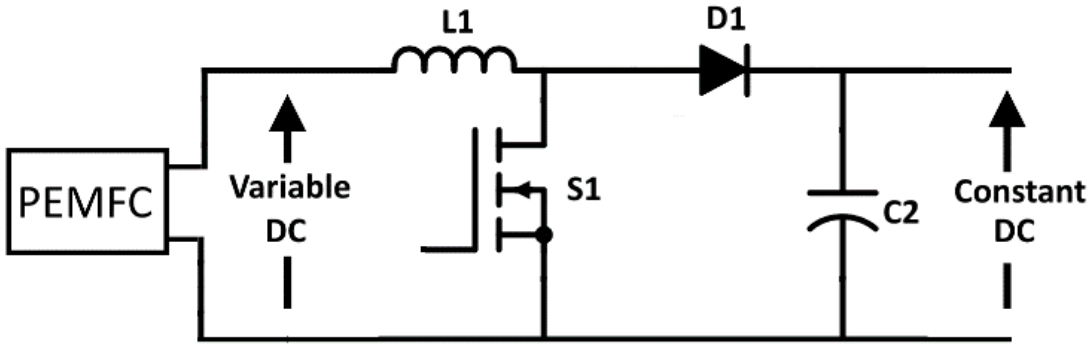

Fig. 2. Conversion stage used to connect the fuel cell to the DC link.

To connect the PEMFC system with the DC link a boost converter has been used. To control this converter, a voltage feedback loop with a PID controller has been implemented, which is responsible for stabilizing the voltage of the DC link. Fig. 3 shows the conversion stage used to couple each PMSG with the DC link.

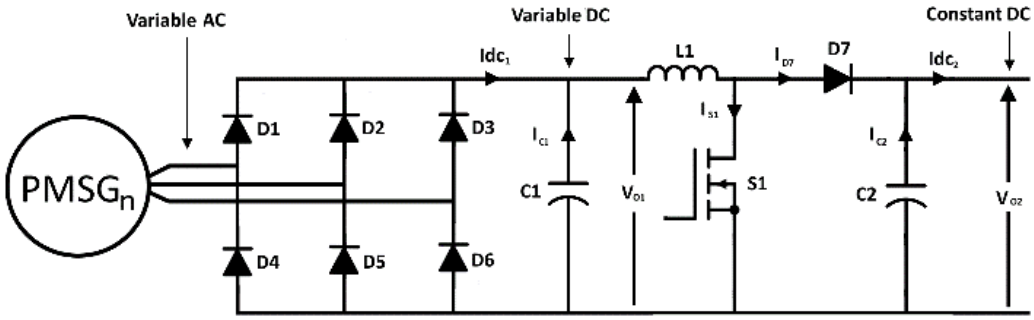

Fig. 3. Conversion stage used to couple each PMSG with the DC link.

The conversion from the PMSGs outputs to the DC link has several stages. First of all, the power generated from the PMSGs of the turbojets is variable both in voltage and frequency, due to variations of the rotational speed of the turbines. In order to overcome these variations, a three-phase full-wave diode bridge rectifier converts the generated power in variable DC. Despite obtaining the generated power in DC, this is not suitable for connecting all the PMSGs in parallel, since it is variable. Therefore, the next step is to convert the variable DC to constant DC by a boost converter. Since the voltage of the DC link is already controlled by the boost converter of the PEMFC, the boost converters of the PMSGs are controlled by feedback current control loops and PID controllers. Besides, the output diodes of the boost converters prevent feedback currents from being produced.

Fig. 4 shows the conversion stage used to couple the DC link to the electrical loads.

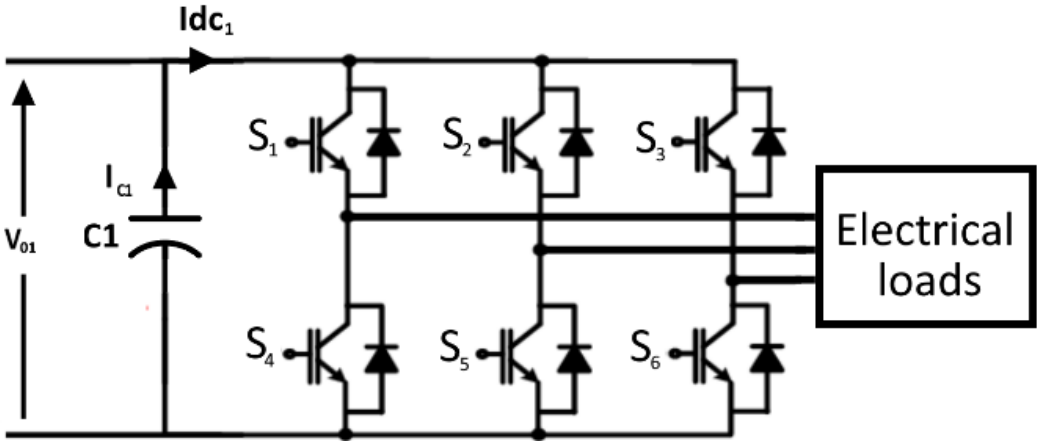

Fig. 4. Conversion stage used to connect the DC link with the electrical loads.

The power conditioning stage to fed the electrical loads from DC link has been implemented with a three-phase IGBT inverter with fixed control switching frequency, established at 400 Hz.

B. System Operation during Taxiing

During taxiing operation mode, the PEMFC system is used to supply the electrical loads of the aircraft using the structure of Fig. 2. Besides, a set of reversible PMSMs located at the landing gear system are used to provide electric traction during taxiing movement of the aircraft. This way, these reversible machines act as motors during taxiing, turning electrical energy into mechanical on the wheels. Fig. 5 shows the conversion stage used to control and fed the PMSMs from the DC link.

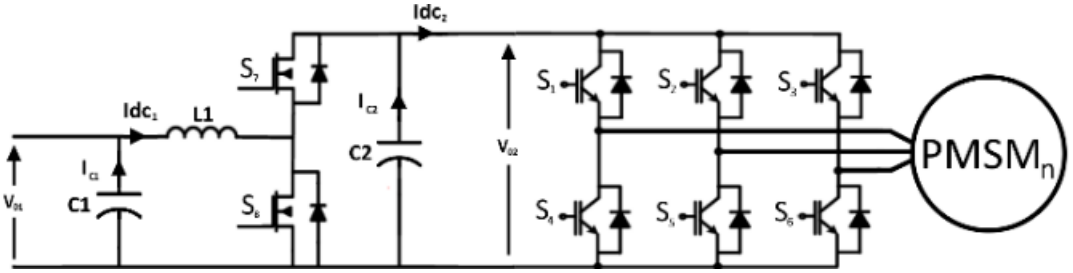

Fig. 5. Conversion stage used to couple each PMSM with the DC link.

The conversion from the DC link to the PMSMs has several stages. First of all, the voltage is reduced through the buck-boost converters, which operate in buck mode. For this, a feedback voltage loop topology has been implemented to control them (switch S_7). After that, a field-oriented control topology is applied to each three-phase IGBT full-bridge inverter to control the PMSMs during the motor mode operation.

The energy needed to supply the PMSMs comes from the Lithium-ion battery, and if this is not enough, it is complemented with the PEMFC system. Thus, maximum efficiency is ensured, since no electrical energy is required from the PMSGs coupled to the turbojets, which operate with very low efficiency in taxiing conditions. Fig. 6 shows the conversion stage used to couple the DC link to the Lithium-ion battery.

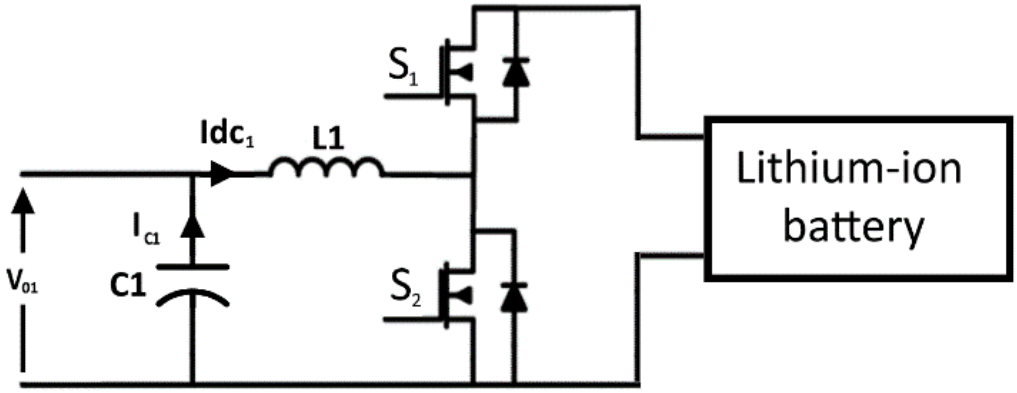

Fig. 6. Conversion stage used to couple the DC link to the battery.

To manage the energy from the Lithium-ion battery, the buck-boost converter is operated in boost mode. For this, a current feedback loop with a PID controller has been implemented in order to control the duty cycle of switch S_2 (Fig. 6).

C. System Operation during Landing

When landing, commonly used strategies require a lot of energy to reduce the speed of the aircraft, which is done mainly by reverse operation of the reactors, aerodynamic braking and mechanical braking. To improve the energy efficiency during landing operation, PMSMs operate as generators, turning the mechanical rotation of the wheels into electrical energy, which is stored in the Lithium-ion cell-based battery for later use in the taxiing operation mode. For this, bidirectional buck-boost converter of the Lithium-ion battery is operated in buck mode. In that case, the converter is controlled by a voltage feedback loop with a PID controller (switch S_1, Fig. 6).

Table 1 summarizes the converter structures and control topologies used to control each generation and storage device, depending on the mode of operation of the aircraft (flight, taxiing, and landing).

TABLE I. SUMMARY OF THE CONVERTER STRUCTURES AND CONTROL TOPOLOGIES DEPENDING ON THE OPERATION MODE.

Device	Converter structure	Operation mode	Control topology
PEMFC	Boost converter	Flight	Voltage feedback loop
		Taxiing	
		Landing	
PMSGs	Three phase full-wave diode bridge rectifiers and boost converters	Flight	Current feedback loop
		Taxiing	
		Landing	
PMSMs		Flight	-

Device	Converter structure	Operation mode	Control topology
	Three-phase IGBT full-bridge inverters and buck-boost converters	Taxiing	Field-oriented control (motor mode) + voltage feedback loop (buck mode)
		Landing	Field-oriented control (generrator mode) + current feedback loop (boost mode)
Battery	Buck-boost converter	Flight	-
		Taxiing	Current feedback loop (boost mode)
		Landing	Voltage feedback loop (buck mode)

IV. SIZING METHODOLOGY

This section describes the sizing methodology used to optimally choose all devices and components of which the microgrid is composed. To guarantee energy production on board, it is decided to design a redundant system composed of two PEMFCs.

Considering the energy needs on board in flight, the hydrogen power P_{h2_f} needed for each PEMFC has been calculated as shown in (1).

$$P_{h2\_f} = 2\frac{P_{fc\_f}}{\eta_{fc}\cdot\eta_{fc\_conv}} \quad (1)$$

where P_{fc_f} is the PEMFC electrical power production in flight [W], η_{fc} is the efficiency of the PEMFC, η_{fc_conv} is the efficiency of the boost converter of the PEMFC, and η_{inv} is the efficiency of the three-phase IGBT inverter used to fed the electrical demand from the DC link. Assuming an average flight time t_f [s], the necessary hydrogen energy E_{h2_f} [J] needed before take-off is obtained in (2).

$$E_{h2\_f} = \frac{P_{h2\_f}\cdot t_f}{\eta_{fc}\cdot\eta_{fc\_conv}\cdot\eta_{inv}} \quad (2)$$

In eq. (3) and (4) the weight of the hydrogen W_{h2_f} [kg] and equivalent weight of jet fuel W_{fuel_f} [kg] needed for the flight are calculated considering the specific hydrogen energy E_{h2_esp} [J/kg] and the specific jet fuel energy E_{fuel_esp} [J/kg], respectively.

$$W_{h2\_f} = \frac{E_{h2\_f}}{E_{h2\_esp}} \quad (3)$$

$$W_{fuel\_f} = \frac{P_{PMSG}\cdot t_f}{\eta_{turb}\cdot\eta_{rec\_dc}\cdot\eta_{PMSG}\cdot\eta_{inv}\cdot E_{fuel\_esp}}\cdot n_{PMSG} \quad (4)$$

Where P_{PMSG} is the PMSG coupled to the turbojets power production in flight [W], n_{PMSG} is the number of PMSGs, η_{turb} is the turbojets efficiency in flight, η_{rec_dc} is the efficiency of the three-phase full-wave diode bridge rectifier and boost converter structure, and η_{PMSG} is the efficiency of the PMSGs. In eq. (5) the total weight saved in the landing gear system $W_{lg\ \_sav}$ [kg] by integrating the in-wheel PMSMs is calculated. For this, it is considered the rim of each wheel weight W_{rim} [kg], the PMSM weight W_{PMSM} [kg], and that wheel covers are not modified. It is supposed that the land gear system is composed of n_{PMSG} PMSMs.

$$W_{lg\ \_sav} = (W_{rim} - W_{PMSM})\cdot n_{PMSG} \quad (5)$$

In eq. (6) it is calculated the kinetic energy required in the taxiing movement E_{tax_mov} [J] has been calculated, while in (7), it is calculated the energy necessary to keep the aircraft in motion E_{fric} [J].

$$E_{tax\_mov} = \frac{1}{2}\cdot W_{\max}\cdot v_{tax}{}^2 \quad (6)$$

$$E_{fric} = \mu_{rod}\cdot\ W_{\max}\cdot g\cdot x_{tax} \quad (7)$$

where $W_{\max}$ is the maximum weight of the aircraft at takeoff [kg], v_{tax} is the taxiing speed [m/s], x_{tax} is the taxiing displacement [m], μ_{rod} is the rolling coeficient, and g is the gravity [m^2/s]. In (8) it is calculated the electrical power P_{tax} [W] to be supplied during the taxiing movement.

$$P_{tax} = \frac{E_{tax\_mov} + E_{fric}}{t_{tax} \cdot \eta_{PMSM} \cdot \eta_{inv_{dc}}} \quad (8)$$

where t_{tax} is the taxiing time [s], η_{PMSM} is the efficiency of the PMSMs, and $\eta_{inv_{dc}}$ is the three-phase IGBT full-bridge inverter and buck-boost structure efficiency. Considering a PEMFC nominal power P_{fc_nom} [W], the electrical power that the two PEMFCs provide in taxiing operation P_{fc_t} [W] has been calculated in (9).

$$P_{fc\_t} = 2 \cdot P_{fc\_nom} \cdot \eta_{fc} \cdot \eta_{fc\_conv} \quad (9)$$

The hydrogen energy E_{h2_t} [J] needed for the taxiing movement during taxiing time t_{tax} is shown in (10), and the weight of the hydrogen W_{h2_t} necessary to generate the energy for the taxiing movement has been calculated in (11).

$$E_{h2\_t} = P_{h2\_t} \cdot t_{tax} \quad (10)$$

$$W_{h2\_t} = \frac{E_{h2\_t}}{\mathrm{E}_{h2\_esp}} \quad (11)$$

Since the power required for the taxiing movement is greater than that provided by the PEMFCs, the extra power P_{bat_t} [W] and energy E_{bat_t} [J] have to be supplied by the batteries, which have been calculated in (12) and (13), respectively.

$$P_{bat\_t} = \frac{P_{tax} - P_{fc\_t}}{\eta_{dc}} \quad (12)$$

$$E_{bat\_t} = P_{bat\_t} \cdot t_{tax} \quad (13)$$

where η_{dc} is the efficiency of the Buck-boost converter of the Lithium-ion battery. Besides, the weight of the jet fuel W_{fuel_t} no longer needed in taxiing mode is shown in (14).

$$W_{fuel\_t} = \frac{(P_{fc\_t} + P_{bat\_t}) \cdot t_{tax}}{\eta_{turb\_t} \cdot E_{fuel\_esp}} \quad (14)$$

where η_{turb_t} is the turbojets efficiency in taxiing operation mode.

The number of Lithium-ion battery cells n_{cells} to be installed in series (n_{series}) and parallel (n_{paral}) depending on cell capacity C_{cell} [Ah] and cell voltage V_{cell} [V], as well as the branch voltage V_{branch} [V] and the battery and branch discharge currents (I_{bat_d} [A], I_{branch_d} [A]) have been calculated in (15-18).

$$n_{cells} = \frac{E_{bat\_t}}{C_{cell} \cdot V_{cell}} \quad (15)$$

$$V_{branch} = n_{series} \cdot V_{cell} \quad (16)$$

$$I_{bat\_d} = \frac{P_{bat\_t}}{V_{branch}} \quad (17)$$

$$I_{branch\_d} = \frac{I_{bat,discharge}}{n_{paral}} \quad (18)$$

The weight of the Lithium-ion battery to be installed W_{bat} [kg] has been calculated in (19), by multiplying the number of cells n_{cells} by the weight of a single cell W_{cell} [kg].

$$W_{bat} = n_{cells} \cdot W_{cell} \quad (19)$$

The total weight of the hydrogen needed W_{h2_tot} [kg] has been calculated in (20), and total weight of the hydrogen tank W_{h2_tank} [kg] once compressed at storage pressure has been calculated in (21).

$$W_{h2\_tot} = W_{h2\_f} + W_{h2\_t} \quad (19)$$

$$W_{h2\_tank} = \frac{W_{h2\_tot} \cdot Vol_{h2\_esp} \cdot F_{comp}}{d_{h2\_tank\_vol} \cdot P_{h2\_tank}} \quad (20)$$

where $Vol_{h2_esp}$is the specific volume of the hydrogen at ambient pressure [m^3/kg], F_{comp} is the compression factor, $d_{h2\_tank\_vol}$ is the tank volume per unit of mass [m^3/kg], and P_{h2_tank} is the tank nominal pressure [Pa].

The weight of the water generated as by-product of the electrochemical reactions is obtained in (21).

$$W_{water} = W_{h2\_tot} \cdot \frac{n_{H_2O}}{n_{H_2}} \quad (21)$$

where n_{h2O} and n_{h2} are the number of moles of water and hydrogen involved in the reactions, respectively.

The energy available at the landing E_{land} [J] which could be recovered by regenerative braking and storage in the battery has been calculated from the general kinetic expression in (22).

$$E_{land} = \frac{1}{2} \cdot m \cdot v_{land}^2 \quad (22)$$

where m and v_{land} are the mass [kg] and the speed [m/s] of the aircraft at the moment of landing, respectively. This kinetic energy can be recovered with a wide range of power outputs which are dependent on the time needed to stop completely the aircraft, which in turn is directly proportional to the desired braking distance. In that case, to choose an optimum braking distance x_{max} [m], an emergency state has been considered based on the following assumptions:

- Reverse thrust in turbojets and disc brakes in wheels are disabled.
- Aerodynamical devices such as flaps are disabled.

Furthermore, to obtain the maximum safety braking distance, coefficients *A* and *B* are calculated in (23) and (24), respectively.

$$A = g \cdot \left(\frac{T_0}{W} - \mu_{rod}\right) \quad (23)$$

$$B = \frac{g}{W} \cdot \left[\frac{1}{2} \cdot \rho \cdot S \cdot (C_D - \mu_{rod} \cdot C_L) + \alpha\right] \quad (24)$$

where T_0 is the thrust [N], W is the maximum landing weight [N], ρ is the mean density of the air [kg/m^3], S is the wings surface [m^2], C_D is the drag coefficient of the aircraft, C_L is the lift coefficient of the aircraft, and α is the relation between the actual thrust and the thrust when the wind speed is zero, which corresponds to zero in landing operation.

In (25) it is calculated the maximum safety braking distance x_{max} considering the aerodynamic parameters of the aircraft and the friction of the wheels with the ground.

$$x_{max} = \frac{1}{2 \cdot B} \cdot \ln\left(\frac{A - B \cdot v_{land}^2}{A}\right) \quad (25)$$

From the previously calculated E_{land} energy available at landing, the global coefficient of friction μ_{tot} that not only represents the coefficient of friction between the wheels and the ground but also represents the friction between the jet and the air, is calculated in (26).

$$\mu_{tot} = \frac{E_{land}}{m \cdot g \cdot x_{max}} \quad (26)$$

Kinematic laws expressed in (27) and (28) are used to calculate the new values of acceleration a and braking time t depending on braking distance x.

$$x = x_0 + v_{land} \cdot t + \frac{1}{2} \cdot a \cdot t^2 \quad (27)$$

$$v = v_{land} + a \cdot t \quad (28)$$

Braking is disabled when the speed v decreases to 10.29 m/s, which is the taxiing speed at which an aircraft commonly moves along the runway [15]. The mechanical power P_{mec} [W] necessary to stop the aircraft is obtained in (29).

$$P_{mec} = \frac{E_{land} - \mu_{tot} \cdot m \cdot g \cdot x_{max}}{t} \quad (29)$$

Considering all the weights added W_{added} to the aircraft (30), and all the weights saved W_{saved} (31), the optimized weight W_{opt} can be obtained, as it is expressed in (32).

$$W_{added} = W_{h2\_tot} + W_{bat} + W_{fc} + W_{h2\_tank} + W_{conv} \quad (30)$$

$$W_{saved} = \mathrm{W}_{\mathrm{lg}\ \_sav} + W_{fuel\_f} + W_{fuel\_t} + W_{water} \quad (31)$$

$$W_{opt} = W_{added} - W_{saved} \quad (32)$$

V. Simulation Results

This section presents the simulation results after evaluating the proposed sizing and operation methodology in a commercial airplane. For this case, the Boeing 747 airplane has been selected, as it is a widely used aircraft and data can be obtained easily. As an example, Fig. 7 shows the DC link voltage, the battery current (charging), as well as the rotation speed of the PMSMs during the landing operation.

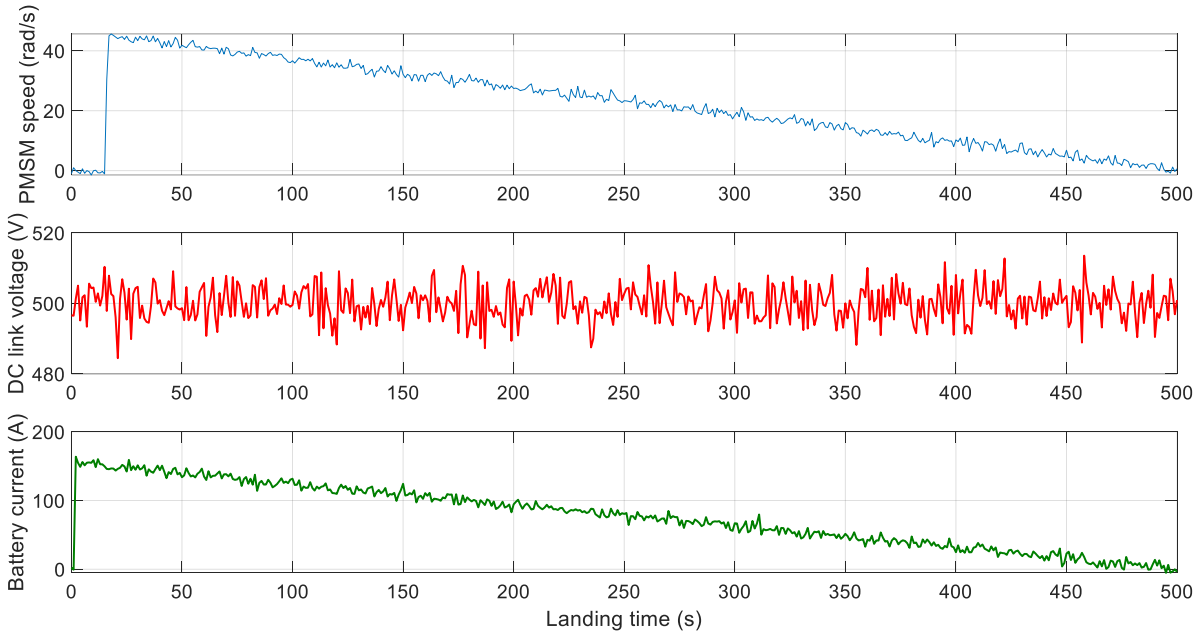

Fig. 7. DC link voltage, baterry current and PMSM speed in landing mode.

As can be seen in Fig. 7, the microgrid has recovered energy for almost 500 s, time in which the airplane has been displaced 5,000 m. The microgrid system has managed correctly the system during the landing of the airplane. In this sense, the DC link voltage has remained constant when charging the battery system from the regenerative energy of the landing gear system. From the total kinetic energy available at the time of landing (674 MJ), it has been recovered the 2.2% through regenerative braking.

Results from a simulation considering the 3 modes of operation in a single trip, have shown that 620 liters of water can be generated. This reduction in weight at takeoff, together with an absolute average improvement in electrical power generation efficiency of 19.59%, represents an approximate kerosene saving of 330 kg per flight.

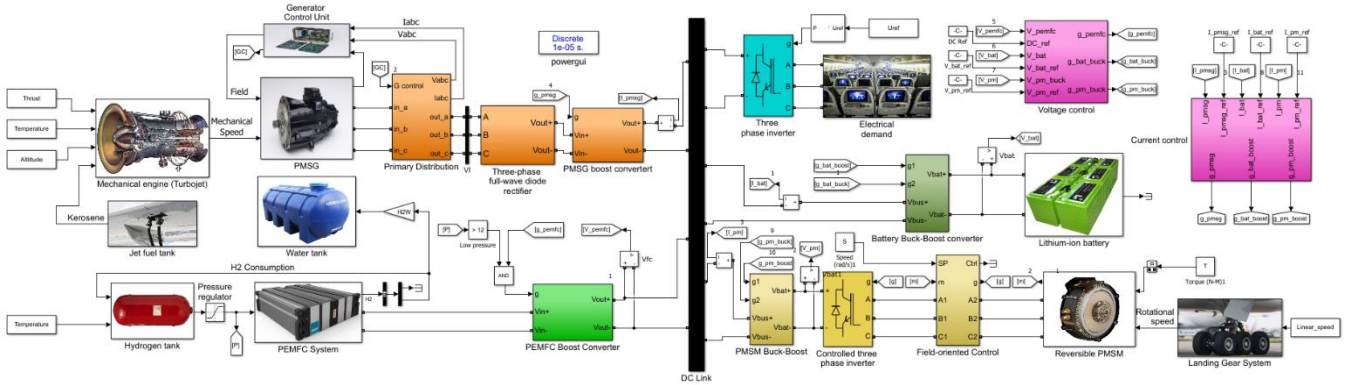

Fig. 8. Configuration of the microgrid in Matlab/Simulink environment.

Fig. 8 shows the configuration of the proposed electrical microgrid in the Matlab/Simulink environment. All electrical generation and storage devices are connected in the DC Link through the corresponding power electronics. The pink boxes

contain the control schemes for all the devices. Table II shows the optimized parameters for commercial devices obtained through the application of the proposed methodology.

TABLE II. MICROGRID CONFIGURATION MAIN PARAMETERS

Parameter	***Value***	***Units***	***Description***
n_{PMSG}	18	-	Number of PMSMs of the landing gear system
P_{fc_nom}	100	kW	PEMFC nominal power
P_{PMSM}	260	kW	PMSM nominal power
$C_{battery}$	552.1	kWh	Lithium-ion battery capacity
$V_{DC\ link}$	500	V	DC link voltage

VI. CONCLUSIONS

This paper focuses on the development of a methodology to optimally operate an electrical microgrid system of an aircraft. The microgrid system is composed of a PEMFC system, PMSMs, PMSGs and a Lithium-ion cell-based battery.

The here proposed design and operation methodology has allowed to optimally choose the number, power and / or capacity of the hydrogen tank, PEMFCs, PMSMs and lithium-ion cells of the battery that allow to minimize the operating costs of the aircraft. A key aspect of the system design lies on the reduction of the weight of the water needed to bring abroad at the moment of taking off. This is possible because it is assumed that the water obtained as by-product of the electrochemical reactions of the PEMFC will be used for sanitary purposes.

In this sense, the optimized microgrid system obtained has allowed a reduction of 370 tons/year in CO_2 emissions due to a reduction in jet fuel consumption. Economically, considering prices for hydrogen of 1.7 €/kg, for kerosene of 1,76 €/gallon, and for electricity of 0.0144 €/kWh, there would be a net savage of 14,070 €/year per airliner in terms of fuel without practically altering the total weight of the airplane.

ACKNOWLEDGMENT

The authors thank the support from the Basque Government (GISEL Research Group IT1191-19 and Project PIBA 2019-98), as well as from the University of the Basque Country UPV-EHU (GISEL Research Group GIU18/181, Project PES17/08 and Project COLAB19/02).

REFERENCES

[1] R. A. Bernabeo et al, "The impact of climate change and weather on air transport in the UAE: Reduction of CO2 emissions," in 2018 Advances in Science and Engineering Technology International Conferences (ASET), 2018, . DOI: 10.1109/ICASET.2018.8376810.

[2] K. Ranasinghe et al, "Review of advanced low-emission technologies for sustainable aviation," Energy, vol. 188, pp. 115945, 2019. . DOI: https://doi.org/10.1016/j.energy.2019.115945.

[3] (03/06/2020). International Councial on Clean Transportation. Available: https://theicct.org/.

[4] (03/06/2020). International Civil Aviation Organization. Available: https://www.icao.int/.

[5] (03/06/2020). International Energy Agency. Available: https://www.iea.org/.

[6] T. Modeer et al, "Design of a GaN-based Interleaved 9-level Flying Capacitor Multilevel Inverter for Electric Aircraft Applications," IEEE Transactions on Power Electronics, pp. 1-1, 2020. . DOI: 10.1109/TPEL.2020.2989329.

[7] H. Gui et al, "Development of High-Power High Switching Frequency Cryogenically Cooled Inverter for Aircraft Applications," IEEE Transactions on Power Electronics, vol. 35, (6), pp. 5670-5682, 2020. . DOI: 10.1109/TPEL.2019.2949711.

[8] S. Gangavarapu and A. K. Rathore, "A Three-Phase Single-Sensor based Cuk-derived PFC Converter with Reduced Number of Components for More Electric Aircraft," IEEE Transactions on Transportation Electrification, pp. 1-1, 2020. . DOI: 10.1109/TTE.2020.2988154.

[9] L. Piscini et al, "Contribution on AC bar windings losses reduction for a high frequency and high performance machine for aeronautical application," in 2019 19th International Symposium on Electromagnetic Fields in Mechatronics, Electrical and Electronic Engineering (ISEF), 2019, . DOI: 10.1109/ISEF45929.2019.9097026.

[10] K. Ozaki et al, "Conceptual Design of Superconducting Induction Motors Using REBa2Cu3Oy Superconducting Tapes for Electric Aircraft," IEEE Transactions on Applied Superconductivity, vol. 30, (4), pp. 1-5, 2020. . DOI: 10.1109/TASC.2020.2971671.

[11] T. Zhao, S. Wu and S. Cui, "Multiphase PMSM with Asymmetric Windings for More Electric Aircraft," IEEE Transactions on Transportation Electrification, pp. 1-1, 2020. . DOI: 10.1109/TTE.2020.2997609.

[12] Y. Wang et al, "Adaptive Online Power Management for More Electric Aircraft with Hybrid Energy Storage Systems," IEEE Transactions on Transportation Electrification, pp. 1-1, 2020. . DOI: 10.1109/TTE.2020.2988153.

[13] F. J. Asensio et al, "Analysis of electrochemical and thermal models and modeling techniques for polymer electrolyte membrane fuel cells," Renewable and Sustainable Energy Reviews, vol. 113, pp. 109283, 2019. . DOI: https://doi.org/10.1016/j.rser.2019.109283.

[14] I. Zamora et al, "Control optimization of an electric traction bus powered by PEMFC and PV," in 2013 IEEE Grenoble Conference, 2013, . DOI: 10.1109/PTC.2013.6652454.

[15] (04/06/2020). Airlines for America. Available: https://www.airlines.org/.